PERGAMON

International Journal of Heat and Mass Transfer 44 (2001) 2385–2394

International Journal of HEAT and MASS TRANSFER

www.elsevier.com/locate/ijhmt

Laminar forced convection in a channel with a moving block

Wu-Shung Fu *, Wen-Wang Ke, Ke-Nan Wang

Department of Mechanical Engineering, National Chiao Tung University, 1001 Ta Hsueh Road, Hsinchu 30050, Taiwan

Received 12 April 2000; received in revised form 12 September 2000

Abstract

Heat transfer rate in a channel with an insulated moving block on a heated surface was studied numerically. For enhancing the heat transfer rate of the heated surface, the block moves back and forth on the heated surface. Then the thermal boundary layer attached to the heated surface is destroyed by the moving block and a new thermal boundary layer reforms immediately as the block passes through. Consequently, a remarkable heat transfer enhancement of the heated surface is attained. This subject belongs to a kind of moving boundary problems, and the modified Arbitrary Lagrangian Eulerian method is suitable for solving this subject. The results show that the maximum increment of heat transfer rate is about 98% in the study.

1. Introduction

Up to now, numerous methods have been proposed to enhance heat transfer rate of a heated body. These methods which mainly include passive and active methods were summarized and reviewed in detail by Bergles [1,2]. However, accompanying with the progress of semiconductor technology, the smaller and more compact devices are produced indefatigably. The heat generated by the new devices is always several times of the former ones and this becomes the main defect of the failure of the devices. As a result, how to increase the heat transfer rate of the heated devices becomes a very important issue.

A method of a channel or pipe installed with ribs is often used to enhance the heat transfer rate of the channel or pipe. A number of studies such as Sparrow et al. [3] and Braaten and Patankar [4] investigated this issue, and the results showed that the ribs disturbed the flow field and enlarged the heat transfer area that caused the increment of the heat transfer rate. Liou et al. [5] investigated experimentally the variations of the mean velocity and turbulence intensity of the channel flow by mounting two pairs of turbulence promoters in tandem. The results showed that the rib pitch-to-height ratio affected the phenomena of separation, reattachment and heat transfer rate. Lin and Hung [6] studied the transient forced convection in a vertical rib-heated channel with a turbulence promoter, and found that the utilization of a turbulence promoter could effectively improve the heat transfer performance in the fully developed region. Iyer and Kakac [7] investigated heat transfer in a channel with periodic grooves to simulate electronic components numerically, and found that beyond a critical Reynolds number, the fluid developed a flow pattern of large-amplitude, time-periodic and nonlinear oscillation. The oscillations enhanced the heat transfer rate of the heated walls. Hwang [8] conducted an experiment to investigate the heat transfer in a rectangular duct of which one wall was roughened by slit or solid ribs. The results showed that the slit ribs provided a better thermal performance under a constant friction power. Wu and Perng [9] studied a numerical investigation on heat transfer enhancement in a horizontal block-heated channel by the installation of an oblique plate. The maximum increase of averaged Nusselt number was 39.5% when the oblique angle was $\pi/3$.

From the above literature, due to the existence of the ribs, the phenomena of separation and reattachment occurred in the flow field which caused the heat transfer in the circulation zone to be complex and small. Then, the increment of heat transfer rate of the channel flow

* Corresponding author. Tel.: +886-3-5712121 ext.55110; fax: 886-3-5720634.

E-mail address: wsfu@cc.nctu.edu.tw (W.-S. Fu).

0017-9310/01/$ - see front matter
PII: S0017-9310(00)00302-1

Nomenclature

b	dimensional width of the block (m)
h	dimensional height of the block (m)
H	dimensional height of the channel (m)
L	dimensional length of the channel (m)
l	dimensional length of the wall (m)
n	the normal vector of surface
Nu	Nusselt number
p	dimensional pressure (N m^{-2})
p_∞	dimensional reference pressure (N m^{-2})
P	dimensionless pressure
Pr	Prandtl number
Re	Reynolds number
t	dimensional time (s)
T	dimensional temperature (K)
u, v	dimensional velocities in x and y directions (m s^{-1})
U, V	dimensionless velocities in X and Y directions
x, y	dimensional Cartesian coordinates (m)
X, Y	dimensionless Cartesian coordinates

Greek symbols

α	thermal diffusivity (m^2 s^{-1})
δ	dimensional boundary layer thickness (m)
θ	dimensionless temperature
λ	penalty parameter
v	kinematic viscosity (m^2 s^{-1})
ρ	dimensional density (kg m^{-3})
τ	dimensionless time

Subscripts

0	airflow inlet
1	inlet channel
3	outlet channel
b	block
h	heated surface
x	local

Superscripts

$-$	mean value
$\wedge$	grid

seems to have limitation by using the above passive methods.

Therefore, the aim of the study is to propose a new method for increasing heat transfer rate of a heated surface in a channel. This method uses a thin block which can move back and forth on the heated surface. The original boundary layers on the heated surface are then destroyed by the moving thin block and the new ones reform right after. Consequently, the huge enhancement of the heat transfer rate of the heat surface of the channel can be attained.

The subject mentioned above belongs to a kind of moving boundary problems, and the Arbitrary Lagrangian Eulerian (ALE) method modified by Fu and Yang [10] is suitably adopted to solve this problem. The results show that the boundary layer is destroyed as the block passes through and the new boundary layer reforms right after. Based upon the reformation of the new boundary layer, a remarkable enhancement of heat transfer is then obtained.

2. Physical model

The physical model is shown in Fig. 1. A horizontal channel with length L and height H is used to simulate the two-dimensional flow channel. The fully developed air, of which the temperature is T_0, flows into the channel from the inlet AB, and exits form the outlet CD. The temperature of the heated surface EF with length l_h is T_h which is higher than T_0. The other surfaces of the channel (surfaces AD, BE and FC) are insulated. An

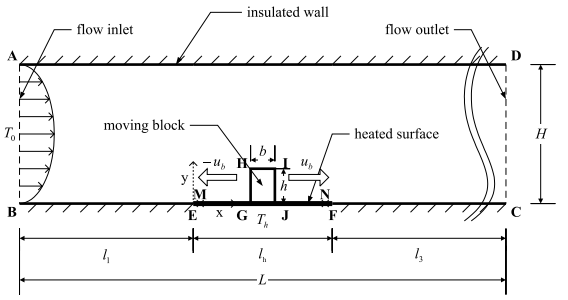

Fig. 1. Physical model.

insulated moving block GHIJ with height h and width b is set on the heated surface and moves back and forth from the positions M to N with a constant velocity u_b.

Initially ($t = 0$), the block is stationary at the middle of the heated surface, and the flow field in the channel is steady. As the time $t > 0$, the block starts to move along the MG line on the heated surface with the constant velocity $-u_b$. When the left surface GH of the block reaches the left point M, the block turns back instantly and moves to the right side with the constant velocity u_b. Similarly, when the right surface IJ of the block reaches the right point N, the block turns back immediately and moves to the left side with the constant velocity $-u_b$. The reciprocation motion of the block mentioned above is continuously executed on the region MN. Then, the original boundary layer on the heated surface is destroyed by the moving block and a new boundary layer reforms right after as the block passes through. Conse-

quently, the behavior of both the flow and thermal fields becomes time-dependent and can be categorized into a kind of moving boundary problem. As a result, the ALE method is properly utilized to analyze this problem.

To simplify the analysis, the following assumptions and the dimensionless variables are made.

1. The flow field is two-dimensional and laminar.
2. The fluid is Newtonian and incompressible.
3. The fluid properties are constant.
4. The no-slip condition is held on the interface between the fluid and block.
5. The effect of gravity is neglected.

$$X=\frac{x}{H},\quad Y=\frac{y}{H},\quad U=\frac{u}{\bar{u}_0},\quad V=\frac{v}{u_0},$$
$$\hat{U}=\frac{\hat{u}}{\bar{u}_0},\quad U_{\mathrm{b}}=\frac{u_b}{\bar{u}_0},\quad P=\frac{p-p_\infty}{\rho\bar{u}_0^2},\quad \tau=\frac{t\bar{u}_0}{H},\qquad (1)$$
$$\theta=\frac{T-T_0}{T_h-T_0},\quad Re=\frac{\bar{u}_0 H}{v},\quad Pr=\frac{v}{\alpha},$$

where $\bar{u}_0$ is the mean velocity of the inlet velocity distribution.

Based upon the above assumptions and dimensionless variables, the dimensionless ALE governing Eqs. (2)–(5) are expressed as the following equations:

Continuity equation

$$\frac{\partial U}{\partial X}+\frac{\partial V}{\partial Y}=0. \qquad (2)$$

Momentum equations

$$\frac{\partial U}{\partial \tau}+(U-\hat{U})\frac{\partial U}{\partial X}+V\frac{\partial U}{\partial Y}=-\frac{\partial P}{\partial X}+\frac{1}{Re}\left(\frac{\partial^2 U}{\partial X^2}+\frac{\partial^2 U}{\partial Y^2}\right), \qquad (3)$$

$$\frac{\partial V}{\partial \tau}+(U-\hat{U})\frac{\partial V}{\partial X}+V\frac{\partial V}{\partial Y}=-\frac{\partial P}{\partial Y}+\frac{1}{Re}\left(\frac{\partial^2 V}{\partial X^2}+\frac{\partial^2 V}{\partial Y^2}\right). \qquad (4)$$

Energy equation

$$\frac{\partial \theta}{\partial \tau}+(U-\hat{\mathrm{U}})\frac{\partial \theta}{\partial X}+V\frac{\partial \theta}{\partial Y}=\frac{1}{PrRe}\left(\frac{\partial^2 \theta}{\partial X^2}+\frac{\partial^2 \theta}{\partial Y^2}\right). \qquad (5)$$

As $\tau>0$, the boundary conditions are as follows:

On the surfaces AD, BE and FC,

$$U=V=0,\quad \partial\theta/\partial n=0. \qquad (6)$$

On the inlet surface AB

$$U=-6\left(Y^2-Y\right),\quad V=0,\quad \theta=0. \qquad (7)$$

On the heated surfaces EG and JF,

$$U=V=0,\quad \theta=1. \qquad (8)$$

On the outlet surface CD,

$$\partial U/\partial n=\partial V/\partial n=\partial\theta/\partial n=0. \qquad (9)$$

On the surfaces of the block GH, HI and IJ

$$U=U_{\mathrm{b}},\quad V=0,\quad \partial\theta/\partial n=0. \qquad (10)$$

3. Numerical method

A Galerkin finite element method with moving mesh is adopted to solve the governing Eqs. (2)–(5). A backward scheme is used to deal with the time-differential terms in the governing equations. A penalty function and Newton–Raphson iteration algorithm are utilized to reduce the pressure and nonlinear terms in the momentum equations, respectively. The velocity and temperature terms are expressed as quadrilateral and nine-node quadratic isoparametric elements. The discretization processes of the governing equations are similar to those used in Fu and Yang [10]. Then, the momentum Eqs. (3) and (4) can be expressed as follows:

$$\sum_1^{n_e}\left([A]^{(e)}+[K]^{(e)}+\lambda[L]^{(e)}\right)\{q\}^{(e)}_{\tau+\Delta\tau}=\sum_1^{n_e}\{f\}^{(e)} \qquad (11)$$

in which

$$\left(\{q\}^{(e)}_{\tau+\Delta\tau}\right)^{\mathrm{T}}=\langle U_1,U_2,\ldots,U_9,V_1,V_2,\ldots,V_9\rangle^{m+1}_{\tau+\Delta\tau}, \qquad (12)$$

where $[A]^{(e)}$ includes the (m)th iteration values of U and V at time $\tau+\Delta\tau$, $[K]^{(e)}$ the shape function, $\hat{U}$ and time differential terms, $[L]^{(e)}$ the penalty function terms, and $\{f\}^{(e)}$ includes the known values of U and V at time τ and (m)th iteration values of U sand V at time $\tau+\Delta\tau$.

After the flow field is solved, the energy Eq. (5) can be expressed as follows:

$$\sum_1^{n_e}\left([M]^{(e)}+[Z]^{(e)}\right)\{c\}^{(e)}_{\tau+\Delta\tau}=\sum_1^{n_e}\{r\}^{(e)}, \qquad (13)$$

where

$$\left(\{c\}^{(e)}_{\tau+\Delta\tau}\right)^{\mathrm{T}}=\langle\theta_1,\theta_2,\ldots,\theta_9\rangle_{\tau+\Delta\tau} \qquad (14)$$

in which $[M]^{(e)}$ includes the values of U and V at time $\tau+\Delta\tau$, $[Z]^{(e)}$ the shape function, $\hat{U}$ and time differential terms and $\{r\}^{(e)}$ includes the known values of θ at time τ.

The value of penalty parameter used in the present study is 10^6 and the frontal method solver is utilized to solve Eqs. (11) and (13). The value of Prandtl number is 0.71 for air. The mesh velocity $\hat{U}$ is in linear distribution and inversely proportional to the distance between the nodes and the moving block.

A brief outline of the solution procedure is described as follows:

1. Determine the optimal mesh distribution and numbers of the elements and the nodes.
2. Solve the values of the U, V and θ at the steady state and regard them as the initial values.
3. Determine the moving velocity U_{b} of the block, the time increment $\Delta\tau$ and the mesh velocity $\hat{U}$ of every node.
4. Update the coordinates of the nodes and examine the determinant of the Jacobian transformation matrix to ensure the one-to-one mapping to be satisfied

during the Gaussian quadrature numerical integration, otherwise execute the mesh reconstruction.

5. Solve Eq. (11), until the following criteria for convergence are satisfied:

$$\left|\frac{\varphi^{m+1}-\varphi^{m}}{\varphi^{m+1}}\right|_{\tau+\Delta\tau} < 10^{-3}, \quad \text{where} \quad \varphi = U \text{ and } V. \tag{15}$$

6. Determine the factors in Eq. (13) by U and V, and solve Eq. (13).
7. Continue the next time-step calculation until the assigned motion of the block has finished.

For the thermal field, the energy balance is checked for every time step by the following equation:

$$E(\%) = \left[\left\{\int_{\mathrm{EF}} Nu_x^{n+1}\,\mathrm{d}X - \int_{\mathrm{CD}} Pr\cdot Re\cdot U^{n+1}\cdot\theta^{n+1}\,\mathrm{d}Y - (Pr\cdot Re\cdot A\cdot(\bar{\theta}^{n+1}-\bar{\theta}^{n}))/\mathrm{d}\tau\right\} \Big/ \int_{\mathrm{EF}} Nu_x^{n+1}\,\mathrm{d}X\right]\times 100, \tag{16}$$

where $\int_{\mathrm{EF}} Nu_x^{n+1}\,\mathrm{d}X$ is the thermal energy added into the system from the heated surface, $\int_{\mathrm{CD}} Pr\cdot Re\cdot U^{n+1}\cdot\theta^{n+1}\,\mathrm{d}Y$ the thermal energy leaving the system with the fluid, and $Pr\cdot Re\cdot A\cdot(\bar{\theta}^{n+1}-\bar{\theta}^{n})/\mathrm{d}\tau$ is the increment of the internal energy of the fluid.

The dimension of the channel and the distribution of mesh are tested under $Re = 100$ and $U_{\mathrm{b}} = 2$, and the non-dimensional time intervals $\Delta\tau$ are tested under every Reynolds number and block moving velocity. For economizing computational time, the length of the inlet channel l_1, the heated surface l_{h}, the outlet channel l_3, the width and the height of the block are chosen as $3H$, H, $20H$, $0.1H$ and $0.2H$, respectively, and the mesh with 114×34 elements is chosen for computations. In addition, the values of non-dimensional time intervals $\Delta\tau$ are chosen at the range from 1×10^{-3} to 4×10^{-3}.

4. Results and discussion

For clearly indicating the phenomena around the moving block, the flow and thermal fields close to the moving block are illustrated only in the following figures. The variations of the velocities, isothermal lines and local Nusselt numbers Nu_x under $Re_j = 500$, and $U_{\mathrm{b}} = 1.0$ are indicated in Figs. 2–4, respectively. The local Nusselt number Nu_x is defined as the follow equation.

$$Nu_x = -\frac{\partial\theta}{\partial \mathrm{Y}}|_{Y=0}. \tag{17}$$

These phenomena shown in Figs. 2–4 are in a certain period of total reciprocation motions. In this period, the variations of the velocity and thermal fields become cyclical.

In Fig. 2(a), the block is on the way to the left, and the position of block is at the center of the heated surface at this moment. The fluid before the moving block flows to the left because the fluid is pushed by the block. However, the main stream in the channel flows to the right and the moving block is regarded as an obstructer. As a result, the velocity of the fluid close to the moving block is much larger than that of the fluid far away from the moving block, and the main flow flows upward to pass the moving block. In the duration of the movement of the block, the moving block destroys the original velocity boundary layer before the moving block.

On the right surface of the block, the fluid complements the vacant space induced by the moving block instantly, and the direction of this fluid is left. As a result, a new velocity boundary layer reforms after the moving block. The values of the velocities in the new boundary layer are larger than those in the original boundary layer shown in the left side of the block apparently, and the increment of the velocity is beneficial to the heat transfer rate of the heated surface.

Fig. 2(b) shows the flow field when the moving block reaches the left point M. The flow field before the moving block in Fig. 2(b) is similar to that shown in Fig. 2(a). However, the recirculation zone behind the moving block is longer than that in Fig. 2(a) and almost covers the heated surface. With the continuous leftward motion of the block, more fluids induced by the moving block flow toward the heated surface and a small recirculation zone forming on the heated surface behind the moving block is observed.

The moving block turns back immediately when the left surface of the block reaches the left point M. In Fig. 2(c), the block is on the way to the right and at the central position of the heated surface. The moving block pushes the fluid near the right surface of the block to flow rightward. However, some fluids in the recirculation zone which forms on the right side of the block flow leftward. Then, the two streams of the fluid mentioned above with different directions interact with each other that causes the interflow to flow upward. On the left side of the moving block, the fluid induced by the moving block and the main stream flow is with the same direction. As a result, more fluids flow toward the heated surface and the boundary layer reforms right behind the moving block.

When the block reaches the right point N, the velocity vectors around the heated surface are shown in Fig. 2(d). With the continuous rightward motion of the block, the block induces more fluids toward the heated surface. The flow fields in Fig. 2(c) and (d) are similar.

In Fig. 2(e), the block reaches the central position of the heat surface again and is on the way to the left. The flow field at this moment is very similar to that shown in

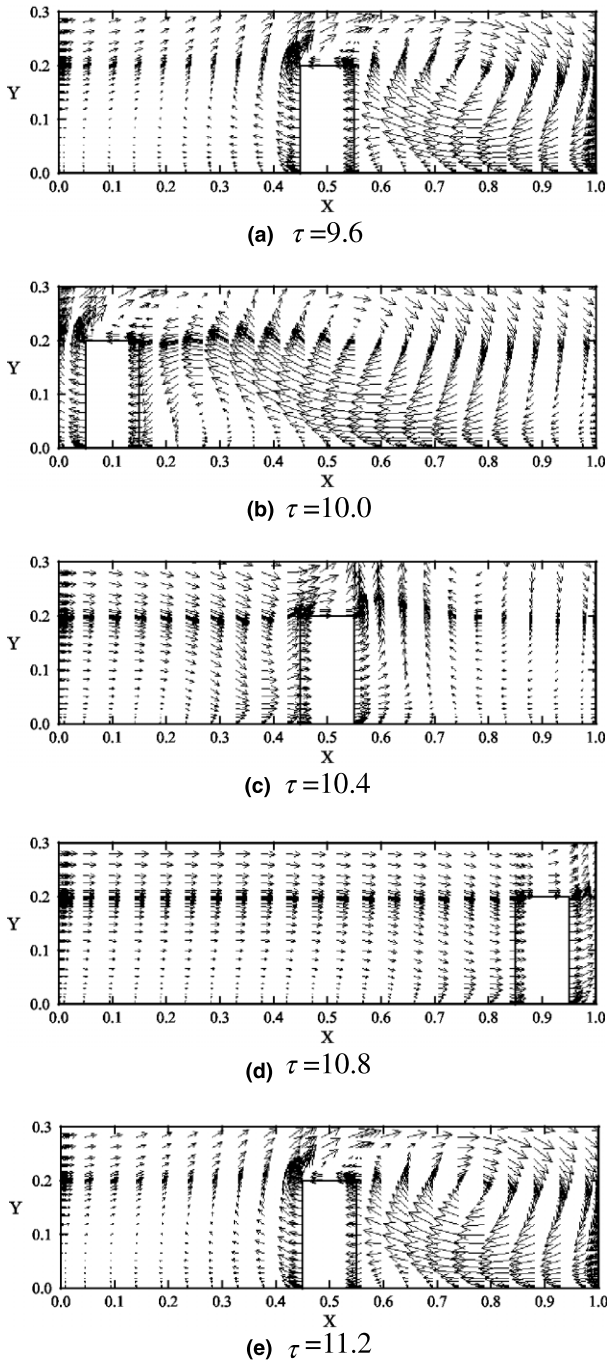

Fig. 2. The velocity vectors near the moving block for $Re = 500$ and $U_b = 1.0$ case.

Fig. 2(a) which indicates the variation of the flow field to be cyclical.

Fig. 3(a)–(e) show the distributions of isothermal lines at the same condition shown in Fig. 2(a)–(e), respectively. The thermal fields are usually in response to the characteristics of the flow fields, and the thermal boundary layer on the heated surface is destroyed by the moving block and reforms right after as the moving block passes through. This results in the distributions of isothermal lines near the front surface of the moving block being spare; however, far away from the moving block the distributions of constant thermal lines are still

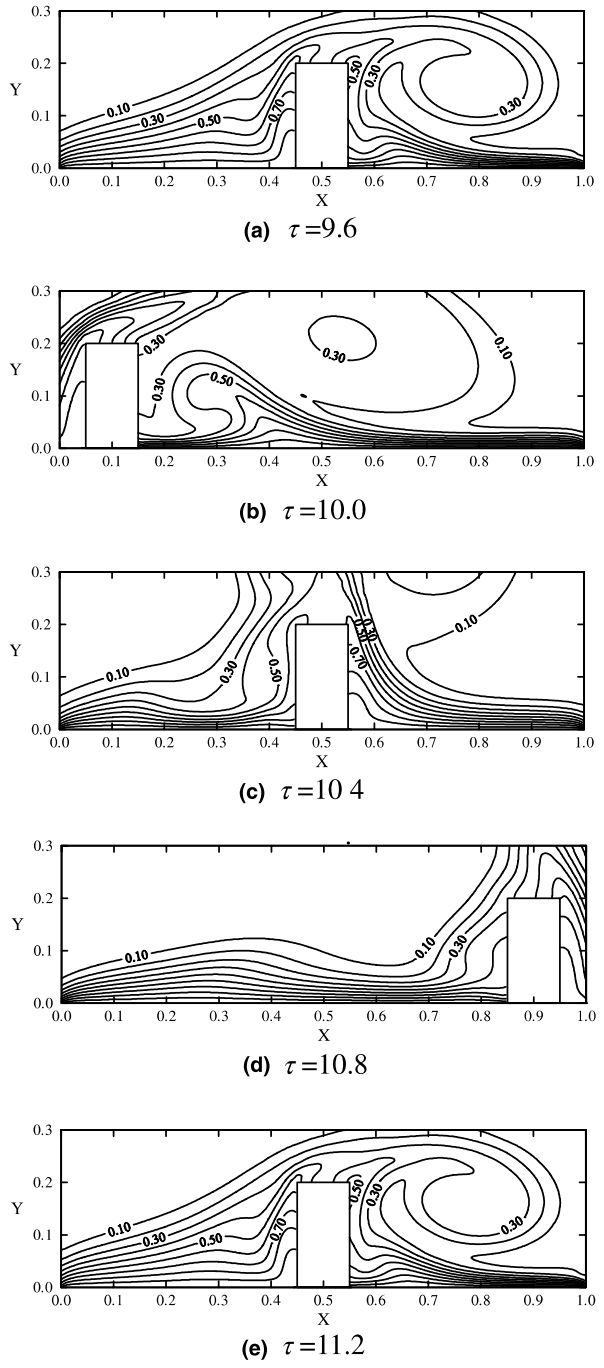

Fig. 3. The isothermal lines near the moving block for $Re = 500$ and $U_b = 1.0$ case.

dense. The new thermal boundary layer reforms after the moving block, the distributions of constant thermal lines are naturally dense which causes the heat transfer of the heated surface to be enhanced remarkably.

The distributions of local Nusselt number Nu_x shown in Fig. 4(a)–(e) are under the same condition as shown in Fig. 3(a)–(e), respectively. The dash lines shown in Fig. 4 indicate the distributions of the local Nusselt number of the heated surface when the channel is without the moving block. The solid lines indicate the distributions of the local Nusselt number of the heated surface when the block is moving. Due to the insulation of the block, the

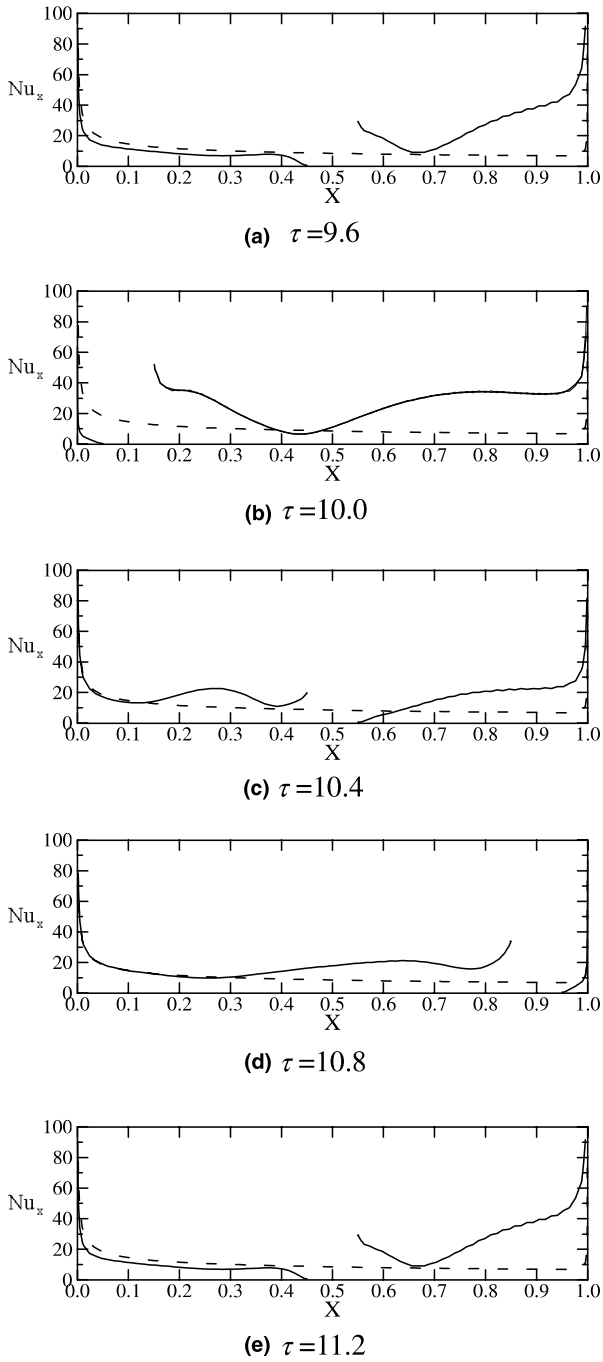

Fig. 4. The Nusselt number distributions on the heated surface for $Re = 500$ and $U_b = 1.0$ case.

distributions of the local Nusselt number shown in these figures are interrupted. The moving block pushes the fluids near the front surface of the moving block directly, which causes the local Nusselt number to become extremely small. Oppositely, a new thermal boundary layer reforms behind the moving block which enlarges the local Nusselt number apparently. Far away from the moving block, the fluid induced by the moving block flows toward the heated surface that is beneficial to the heat transfer rate of heated surface. Consequently, the local Nusselt number of the case with the moving block becomes larger than that of the case without the moving block.

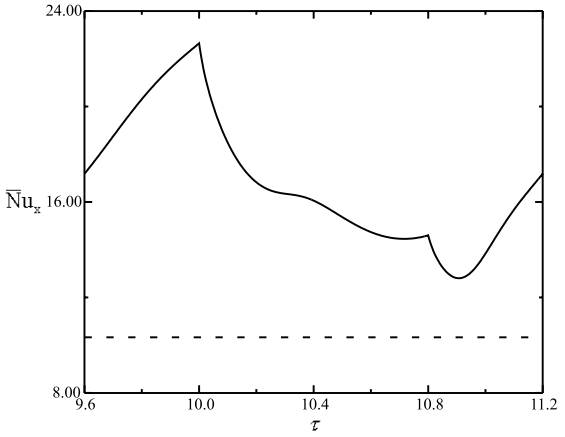

Fig. 5. The variations of the averaged Nusselt number $\bar{N}u_x$ during the τ from 9.6 to 11.2 for $Re = 500$ and $U_b = 1.0$ case.

The variations of the averaged Nusselt number $\bar{N}u_x$ of the heated surface of a certain cycle are shown in Fig. 5. The definition of the averaged Nusselt number $\bar{N}u_x$ is shown in the following equation:

$$\bar{N}u_x = \int_{\text{heated surface}} -\frac{\partial\theta}{\partial Y}|_{Y=0}\,\mathrm{d}X. \tag{18}$$

The dash lines shown in Fig. 5 indicate the distributions of the averaged Nusselt number of the heated surface when the channel is without the moving block.

As the block moves to the left as shown in Fig. 2(a) and (b), the new thermal boundary layer reforms right after the moving block. The recirculation zone behind the moving block induces more low temperature fluids toward the heated surface that causes the averaged Nusselt number to increase continuously (the time interval from 9.6 to 10.0). As the block moves rightward from the left point M (Fig. 2(b)), the local Nusselt number decreases before the block, and the increment of local Nusselt number behind the block is small. Then, the averaged Nusselt number decreases continuously (the time interval from 10.0 to 10.4). As the block passes through the central position of the heated surface and moves continuously to the right, more fluids flow toward the heated surface, and the local Nusselt number behind the block becomes larger. As a result, the decrement of the averaged Nusselt number slows down (the time interval from 10.4 to 10.8).

When the block begins to move leftward from the right point N, the fluid before the block flows to the left by the movement of the block, and prevents the cold fluid flowing toward the heated surface. Moreover, the fluid induced by the block is weak behind the block. Then, the averaged Nusselt number still decreases. With the continuous leftward motion of the block, the new boundary layer zone behind the block becomes larger which leads the averaged Nusselt number to be increment. When the block is at the central position of the heated surface again (Fig. 2(e)), the distribution of the local Nusselt number is similar to that in Fig. 2(a). Then the variations of the averaged Nusselt number become periodic (the time interval from 10.8 to 11.2).

Figs. 6–9 show the variations of averaged Nusselt numbers per unit cycle $\bar{N}u$ on the heated surface with the moving velocity of block being equal to 1.0 and 2.0, and the Reynolds number being equal to 100 and 500, respectively. The averaged Nusselt number per unit cycle is defined as the following equation.

$$\bar{N}u = \frac{1}{m}\sum_{i=1}^{m}\left(\int_{\text{heated surface}} Nu_x\,\mathrm{d}X\right)_i, \tag{19}$$

where m is the number of the time steps per unit cycle. The sign "◆" shown in these figures indicate the aver-

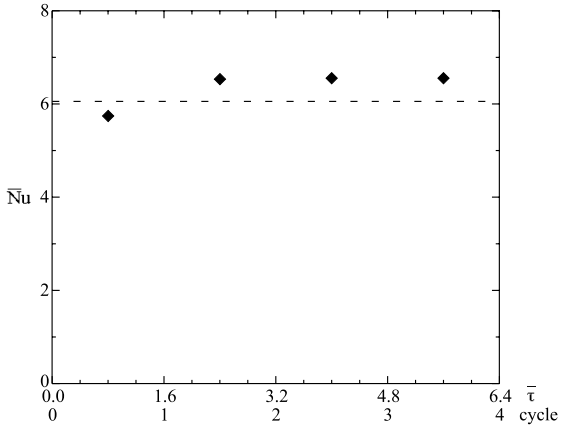

Fig. 6. The variations of averaged Nusselt number per unit cycle $\bar{N}u$ with τ for $Re = 100$ and $U_b = 1.0$ case.

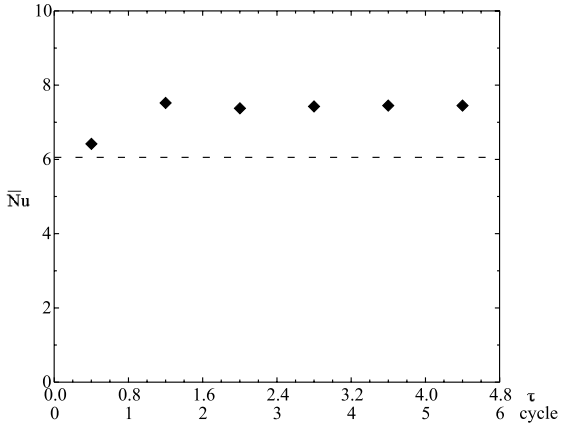

Fig. 7. The variations of averaged Nusselt number per unit cycle $\bar{N}u$ with τ for $Re = 100$ and $U_b = 2.0$ case.

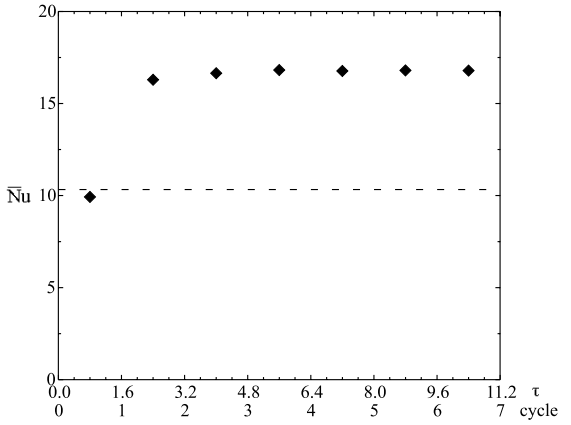

Fig. 8. The variations of averaged Nusselt number per unit cycle $\bar{N}u$ with τ for $Re = 500$ and $U_b = 1.0$ case.

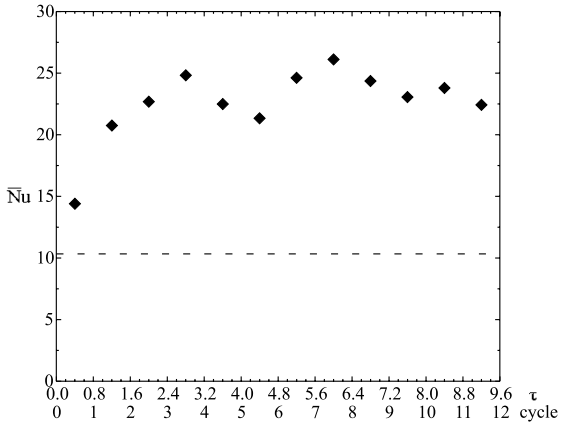

Fig. 9. The variations of averaged Nusselt number per unit cycle $\bar{N}u$ with τ for $Re = 500$ and $U_b = 2.0$ case.

aged Nusselt number per unit cycle $\bar{N}u$, and the dash lines represent the averaged Nusselt number of the heated surface when the channel is without the moving block.

As shown in Fig. 6, except the first cycle, the heated transfer rate increases slightly. In the total duration, the magnitude of enhancement of total heat transfer rate is small and about 8%, this could be that the addition of the insulated moving block decreases the heat transfer area.

Fig. 7 shows the variations of averaged Nusselt number per unit cycle $\bar{N}u$ when the moving velocity of block is 2.0 and the Reynolds number is 100. The moving velocity of block is high enough to destroy the original thermal boundary layer and the new thermal boundary layer reforms right after as the block passes through. Then the increment of the total Nusselt numbers becomes larger and is about 23% in this duration.

When the Reynolds number increases to 500, and the block moves with the velocity $U_b = 1.0$, the variations of the averaged Nusselt number per unit cycle are shown in Fig. 8. The increment of the averaged Nusselt number per unit cycle is about 62.4% after the dimensionless time being equal to 11.2.

In Fig. 9, the block moves with the velocity $U_b = 2.0$ and the Reynolds number is 500. The enhancement of heat transfer rate is about 98% in the case. The variations of the averaged Nusselt number per unit cycle are not periodic, which suggests that the moving velocity of block is too fast and the patterns of the flow and thermal fields do not develop a regular type in time.

5. Conclusions

A numerical investigation of heat transfer of a channel with a block moving back and forth on the heated surface is studied. The main conclusions can be summarized as follows:

1. The modified Arbitrary Lagrangian Eulerian method is suitable for solving the moving boundary problem.
2. The thermal boundary layer on the heated surface is destroyed by the moving block and reforms right after as the block passes through. The reformation of the thermal boundary layer is the main mechanism for enhancing heat transfer of the heated surface.
3. The moving velocity and the position of the block affect the heat transfer of the heated surface remarkably.

Acknowledgements

The support of this work by National Science Council, Taiwan, ROC under contract NSC89-2212-E-009-072 is gratefully acknowledged.

References

[1] A.E. Bergles, Recent development in convective heat-transfer augmentation, Appl. Mech. Rev. 26 (1973) 675–682.
[2] A.E. Bergles, Survey and evaluation of techniques to augment convective heat and mass transfer, Prog. Heat Mass Transfer 1 (1969) 331–424.
[3] E.M. Sparrow, J.E. Nithammer, A. Chaboki, Heat transfer and pressure drop characteristics of arrays of rectangular modules encountered in equipment, Int. J. Heat Mass Transfer 25 (7) (1982) 961–973.
[4] G. Bergeles, N. Athanassiadis, The flow pass a surface-mounted obstacle, J. Fluids Eng. Trans. ASME. 105 (1983) 461–463.
[5] T.M. Liou, Y. Chang, D.W. Hwang, Experimental and computational study of turbulent flows in a channel with

two pairs of turbulence promoters in tandem, J. Fluids Eng. Trans. ASME. 112 (1990) 302–310.
[6] H.H. Lin, Y.H. Hung, Transient forced convection heat transfer in a vertical rib-heated channel using a turbulence promoter, Int. J. Heat Mass Transfer 36 (6) (1993) 1553–1571.
[7] R.S. Iyer, S. Kakac, K.Y. Fung, Instability and heat transfer in grooved channel flow, J. Thermophys. Heat Transfer 11 (3) (1997) 437–445.
[8] J.J. Hwang, Heat transfer–friction characteristic comparison in rectangular ducts with slit and solid ribs mounted on one wall, J. Heat Transfer Trans. ASME. 120 (1998) 709–716.
[9] H.W. Wu, S.W. Perng, Effect of an oblique plate on the heat transfer enhancement of mixed convection over heated blocks in a horizontal channel, Int. J. Heat Mass Transfer 42 (1999) 1217–1235.
[10] W.S. Fu, S.J. Yang, Numerical simulation of heat transfer induced by a body moving in the same direction as flowing fluids, Heat Mass Transfer 36 (2000) 257–264.